Femtotesla Magnetic Field Measurement with Magnetoresistive Sensors

Myriam Pannetier,[1*] Claude Fermon,[1] Gerald Le Goff,[1] Juha Simola,[2] Emma Kerr[3]

The measurement of magnetic fields in the femtotesla (fT, 10^{-15} tesla) range is important for applications such as magnetometry, quantum computing, solid-state nuclear magnetic resonance, and magnetoencephalography. The only sensors capable of detecting these very small fields have been based on low-temperature superconducting quantum interference devices operating at 4.2 kelvin. We present a magnetic field sensor that combines a superconducting flux-to-field transformer with a low-noise giant magnetoresistive sensor. The sensor can be operated up to 77 kelvin. Our small-size prototype provides the capability of measuring 32 fT.

Noninvasive mapping of brain activity can be performed by magnetic resonance imaging (MRI) (*1*) through the change of nuclear relaxation times, or by magnetoencephalography (MEG) (*2*), which directly senses the very small magnetic fields (on the order of a few femtoteslas) in a frequency range of 3 to 30 Hz produced by neural activity. Sensors used for this imaging are typically based on arrays of superconducting quantum interference devices (SQUIDs) with low transition temperatures (T_c) (*3*). The best sensitivity achieved is about 1 fT/Hz$^{1/2}$ for a 1.5-cm^2 loop with low-T_c SQUIDs (*4*) and about 30 fT/Hz$^{1/2}$ with high-T_c SQUIDs (*5*). Although a recent technique based on atomic resonance has been proposed for subfemtotesla resolution (*6*), the required apparatus may be too cumbersome to build up a full array of sensors around the patient's head.

Low-T_c SQUIDS are flux sensitive, whereas magnetoresistive (MR) sensors are field sensitive. The sensitivity of a MR sensor is independent of its size, whereas a SQUID's sensitivity is proportional to its area. The MR sensor becomes competitive for areas smaller than 10 μm^2. In our sensor, in which an efficient flux-to-field transformer and a very sensitive MR sensor are combined, the transformer is made of a superconducting loop containing a micrometer-size constriction. A device with a coplanar Hall sensor has been explored (*7*), but its sensitivity is limited by that of the Hall sensors and by the geometry. The MR sensor is placed or deposited below or on top of the constriction. It measures the applied field amplified by a factor up to a few thousands, depending on the geometry and size of the device.

A GMR (giant magnetoresistance) (*8*) spin valve sensor is made of a hard magnetic layer separated from a soft magnetic film by a thin metallic layer. The magnetization of the soft magnetic layer—usually a NiFe film coupled to a CoFe film—can rotate easily in an in-plane applied field. The hard layer is composed of an antiferromagnetic layer (e.g., IrMn, MnPt) coupled to a thin ferromagnetic layer (CoFe). The resistance of the whole stack varies with the angle between the magnetization axis of the two layers. Variations of resistance of 6 to 8% can be obtained in industrial production conditions on 150-mm wafers. With micrometer-size sensors, MR variation of about 5% per mT can be achieved. In our prototype, we obtain a MR variation of 2.13% per mT. The resistance R of the GMR stack is 270 ohms for our 5-μm-wide prototype. Thermal noise at room temperature is given by $N_T = 2[(k_B TR)^{1/2}]$ (in units of V/Hz$^{1/2}$), which corresponds to a sensitivity of 350 pT/Hz$^{1/2}$ with a sensing current I of 1 mA for our sensor. At 4.2 K, the sensitivity is 40 pT/Hz$^{1/2}$. As we measure a resistance, the signal is proportional to the sensing current. The sensitivity can thus be increased with the use of a higher current within the limit of heating effects.

At low frequency f, GMR sensors also exhibit $1/f$ noise of both structural and magnetic origin. It is globally given (*9*) by $N_{1/f}(f) = (\gamma/N_C f)^{1/2} RI$, where γ is the Hooge constant and N_C is the number of charge carriers in the device. The magnetic noise can be completely suppressed by proper design of the GMR sensor in a yoke-shape with a good length/width ratio (typically 10) (Fig. 1, right panel). With this specific shape of the sensor, the correct thickness of the soft layer, and a very low roughness of each layer, we obtain Hooge constants of about 5×10^{-3} (independent of the applied field) in four-point

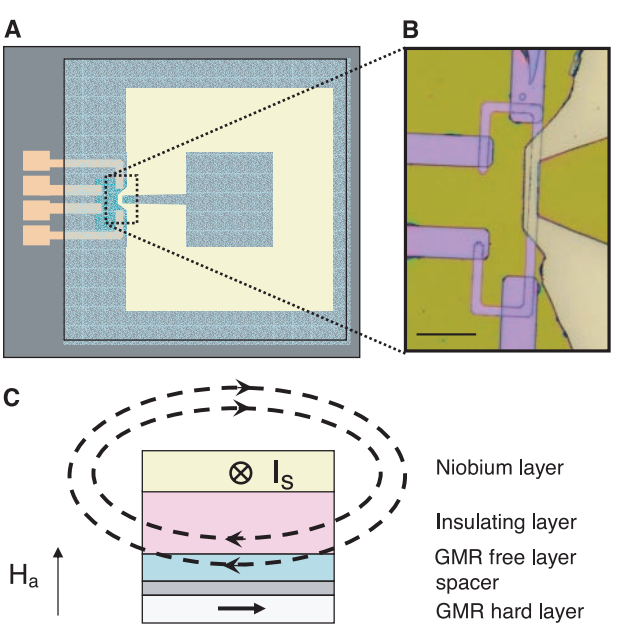

Fig. 1. (**A**) Schematic view of the device, comprising a GMR sensor, measured with four-probe contacts, with a superconducting loop of niobium, electrically isolated from the GMR by 400 nm of Si_3N_4 and closed above the GMR by a constricted area. (**B**) Close-up view of the constriction area. Scale bar, 20 μm. The GMR is patterned in a yoke-type shape of 70 μm length, and titanium contacts allow measurement of the central, domain-free, part. The superconducting constriction is located above the GMR without covering the entire measured part. (**C**) The niobium loop acts as a flux-to-field transformer. The H_a field, applied perpendicular to the plane of the sample, generates in the superconducting loop a supercurrent I_s tending to expel the flux from entering the superconductor as a result of the Meissner effect. The field lines (dashed lines) due to the supercurrent are locally enhanced in the constriction, and their horizontal component can be detected by the GMR sensor positioned under the constriction, according to the direction they give to the free layer magnetization, relative to the hard layer direction (bottom black arrow).

[1]SPEC/DRECAM, Commissariat à l'Energie Atomique Saclay, 91191 Gif-sur-Yvette, France. [2]Elekta Neuromag Oy, P.O. Box 68, FIN-00511 Helsinki, Finland. [3]SFI Laboratory, Physics Department, Trinity College Dublin, Dublin 2, Ireland.

*To whom correspondence should be addressed. E-mail: mp@drecam.saclay.cea.fr

measurements in our samples. Our samples are good metals, so the number of carriers is comparable to the number of atoms.

Flux-to-field transformation is often done with soft magnetic materials designed as flux concentrators, but this solution incurs an extra intrinsic noise. Therefore, we have designed a flux-to-field transformer formed of a large superconducting loop closed by a micrometer-sized constriction (Fig. 1). When an external low-frequency field H_a is applied perpendicular to the superconducting loop, a supercurrent is established to maintain the flux through the loop. If this current flows through a constricted area, its high surface density will lead to a very high coplanar magnetic field above and below the narrow part of the loop. This field can be detected by the GMR sensor, which is sensitive to the in-plane field. The supercurrent can be calculated from the inductance of the ring and the flux screened, or effective area that screens the field (*10*). To maximize the local amplification effect, one needs to use a ring with a large outer diameter and a width of 0.7 times the radius (*11*), as well as a constriction that is as small as possible. A rough estimation of the gain is given by the ratio of the loop radius to the constriction width. A precise calculation of the gain has been done, taking into account the supercurrent distribution in the rectangular constriction (*12*). The results are in agreement with finite-element simulation.

The first experiment was performed on a GMR-Si_3N_4-Nb sample. A commercial GMR stack (*13*) deposited on a silicon substrate was used as the base of the device. The GMR material description, measurement method, and calibration are detailed elsewhere (*14*).

For calibration, the GMR sensor was first measured in a parallel field as function of temperature (fig. S1, inset); fig. S1 gives the resistance from –28 to 28 mT at 5 K. The MR ratio is 9%, and a maximum sensitivity of 2.13% per mT is obtained in the middle of the linear part of the curve. The sample was cooled down below T_c in the corresponding in-plane bias field of 2 mT to ensure that measurements will be done in the most sensitive region. At 4.2 K, the response of the system to a small field H_a is given in Fig. 2. The effective gain of the transformer is 108, given by the ratio between the slope of the GMR in parallel field (2.13% per mT) and the slope for H_a (231% per mT). This ratio does not depend on temperature in the superconducting state. The supercurrent (measured through the field created) reaches a critical value for an applied field of 5.85×10^{-6} T, limiting the parallel field and thus leading to a plateau in the GMR resistance. When one sweeps the field back, the supercurrent decreases to zero and then to negative values up to the critical point in a counterrotating direction. The GMR resistance decreases with the same slope and reaches a low saturation value. The same process is reproduced as soon as the field is swept back to the high saturation value. The inset in Fig. 2 gives the total MR variation as a function of temperature. It decreases with temperature, reaching zero at the critical temperature of the constriction, 6 K, which is lower than the critical temperature of the main loop (8.5 K). The effective gain leads to a sensitivity of 540 fT/Hz$^{1/2}$ with a sensing current of 1 mA (Fig. 3).

Measurement of the intrinsic noise of our system is very difficult, as the thermal noise is about 0.1 nV/Hz$^{1/2}$ and the noise of the preamplifier is about 1 nV/Hz$^{1/2}$. For that reason, we couple our loop to a coil mounted in positive feedback. There are a variety of ways of arranging inductive positive feedback in the readout of dc SQUIDs (*15*–*17*). We have shown that the same methods can also be applied for the readout of the magnetoresistance in our mixed-sensor design. We have tried two different configurations—with the feedback coil coupled either in parallel or in series with the GMR element—with identical outcomes. The data shown in Fig. 3 are taken with the feedback coil coupled in series with the GMR element. Measurements obtained with different feedback amplification are shown in fig. S2.

Mixed sensors with high-T_c superconductors present several advantages: they work at 77 K with a rather good sensitivity; at 4.2 K, they offer a large critical current and very high sensing currents can be applied, up to 15 mA. In a second experiment, we measured a sample with $YBa_2Cu_3O_{7-\delta}$ loop (T_c = 85 K) of comparable size to the niobium one (*14*). Preliminary results have

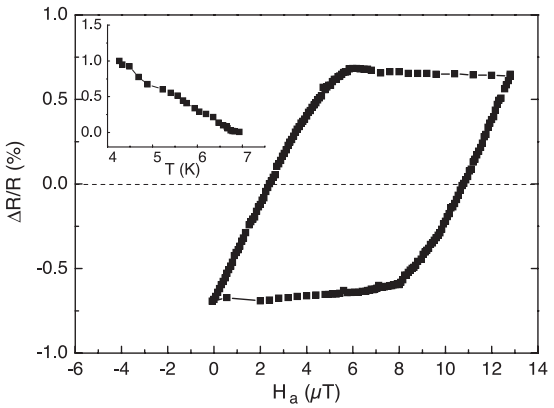

Fig. 2. Magnetoresistance as a function of a perpendicular applied field at 4.9 K. The upper and lower plateaus $(\Delta R/R)_{max}$ correspond to the points where the supercurrent reaches the critical value. The slope corresponds to a resistance variation of 213% per mT, to be compared to 2% per mT with an in-plane applied field (i.e., an enhancement factor of 108 for the flux-to-field transformer). **(Inset:)** Variation of $(\Delta R/R)_{max}$ as a function of temperature. This gives a direct measurement of the critical temperature of the constriction.

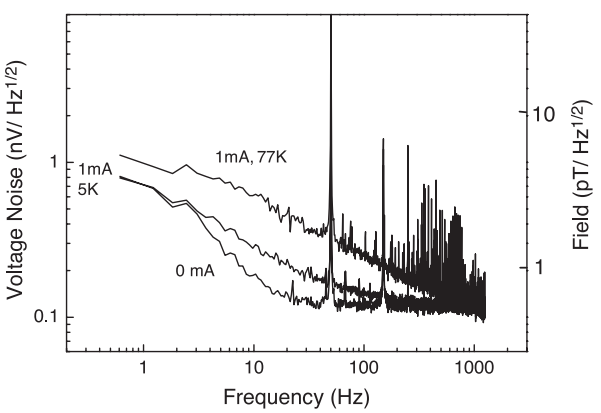

Fig. 3. For the niobium-based device, the noise spectra of the voltage output of the GMR are given with a zero current (lower curve), with 1 mA at 4.2 K (middle curve), and with 1 mA at 77 K (upper curve). The field sensitivity of the device with 1 mA at 4.2 K is given on the scale at the right. At 4.2 K, the 1/*f* noise dominates the thermal noise below 150 Hz.

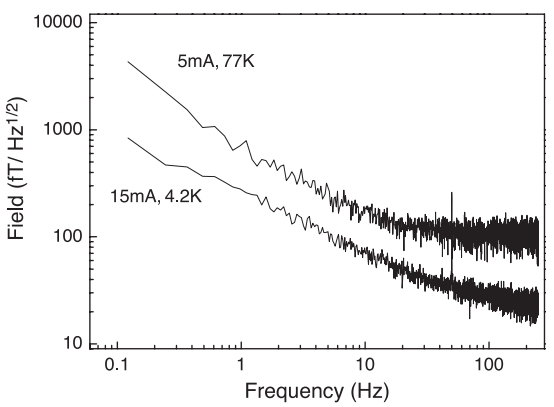

Fig. 4. Noise spectra of the YBaCuO mixed sensor at 4.2 K and 77 K, with 15 mA and 5 mA of sensing current, respectively. At 4.2 K and with a sensing current of 15 mA, the sensitivity of the YBCO device reaches 32 fT/Hz$^{1/2}$, comparable to the noise level of high-temperature SQUIDs.

shown that the behavior is identical to the Nb-loop sensor; the measured gain of 100, constant up to 80 K (fig. S3), is in good agreement with the theoretical predictions (*18*). Figure 4 shows a sensitivity of 32 $fT/Hz^{1/2}$ at 4.2 K (thermal noise) for our high-T_c prototype with a sensing current of 15 mA, which is comparable to the noise level of high-temperature SQUIDs (*5*).

From our results, we can now predict theoretically the potential sensitivity of this new type of sensor. With a constriction of 1 μm and a loop 3 cm in diameter, as used in MEG, the calculated gain is 7500, a factor of 75 higher than in our prototypes. If we use high-T_c superconductors, we can use a sensing current of 5 mA at 77 K. The resistivity of the GMR system with a 1-μm constriction is about 1500 ohms. These values lead to a sensitivity of 1 $fT/Hz^{1/2}$ at 77 K (thermal noise) that should be obtained with a standard GMR sensor. The $1/f$ noise should dominate the thermal noise below 200 Hz. Tunnel magnetoresistance (TMR) sensors (*19*), in which the thin metallic interlayer is replaced by a thin insulator layer acting as a tunnel barrier, can also be used. MR of 50% is currently obtained, leading to a MR variation of 25% per mT. The resistance of the TMR can also be higher on a small surface. If we replace the GMR sensor by a TMR sensor, we achieve a sensitivity of 0.2 $fT/Hz^{1/2}$ at 77 K, a factor of ~5 improvement.

Ultimately, one could use TMR sensors with half-metallic electrodes. This kind of sensor, based on manganite compounds, exhibits low field magnetoresistance of 1800% at 4.2 K (*20*, *21*). They can be epitaxially grown on the high-T_c films, producing a high-quality film. With the proper substrate, manganite films with extremely low $1/f$ noise have been produced (*22*). Such systems should be able theoretically to reach sensitivity around 0.01 $fT/Hz^{1/2}$.

References and Notes

1. G. Dehaene-Lambertz, S. Dehaene, L. Hertz-Pannier, *Science* **298**, 2013 (2002).
2. R. Salmelin, R. Hari, O. V. Lounasmaa, M. Sams, *Nature* **368**, 463 (1994).
3. H. Weinstock, *SQUID Sensors: Fundamentals, Fabrication and Applications* (Kluwer Academic, Dordrecht, Netherlands, 1996).
4. J. Gallop, *Supercond. Sci. Technol.* **16**, 1575 (2003), and references therein.
5. H. J. Barthelmess *et al.*, *IEEE Trans. Appl. Superconduct.* **11**, 657 (2001).
6. I. K. Kominis, T. W. Kornack, J. C. Allred, M. V. Romalis, *Nature* **422**, 596 (2003).
7. S. Linzen *et al.*, *Physica C* **372–376**, 146 (2002).
8. M. N. Baibich *et al.*, *Phys. Rev. Lett.* **21**, 2472 (1988).
9. F. N. Hooge, *Physica B* **83**, 14 (1976).
10. L. D. Landau, E. M. Lifshitz, *Electrodynamics of Continuous Media*, vol. 8 of *Course of Theoretical Physics* (Pergamon, Oxford, 1960).
11. M. Pannetier, C. Fermon, unpublished data.
12. E. H. Brandt, G. P. Mikitik, *Phys. Rev. Lett.* **85**, 4164 (2000).
13. The GMR stack used in the niobium-based device is a commercial one deposited by IPHT (Jena, Germany).
14. See supporting data on *Science* Online.
15. D. Drung, R. Cantor, M. Peters, H. J. Scheer, H. Koch, *Appl. Phys. Lett.* **57**, 406 (1990).
16. H. Seppä, A. Ahonen, J. Knuutila, J. Simola, V. Vilkman, *IEEE Trans. Magn.* **27**, 2488 (1991).
17. Finland Patent 95628, European Patent 0528885, U.S. Patent 5488295, and Japan Patent 3508953.
18. M. Pannetier, C. Fermon, E. Kerr, M. Welling, R. J. Wijngaarden, unpublished data.
19. J. S. Moodera, L. R. Kinder, T. M. Wong, R. Meservey, *Phys. Rev. Lett.* **74**, 3273 (1995).
20. M. Viret *et al.*, *Europhys. Lett.* **39**, 545 (1997).
21. M. Bowen *et al.*, *Appl. Phys. Lett.* **82**, 233 (2003).
22. P. Reutler *et al.*, *Phys. Rev. B* **62**, 11619 (2000).

23. Supported by the European project MAGNOISE, grant IST-1999-10849.

Supporting Online Material

www.sciencemag.org/cgi/content/full/304/5677/1648/DC1
Materials and Methods
Figs. S1 to S3

17 February 2004; accepted 28 April 2004

Ferroelectricity in Ultrathin Perovskite Films

Dillon D. Fong,[1] G. Brian Stephenson,[1*] Stephen K. Streiffer,[1] Jeffrey A. Eastman,[1] Orlando Auciello,[1] Paul H. Fuoss,[1] Carol Thompson[2]

Understanding the suppression of ferroelectricity in perovskite thin films is a fundamental issue that has remained unresolved for decades. We report a synchrotron x-ray study of lead titanate as a function of temperature and film thickness for films as thin as a single unit cell. At room temperature, the ferroelectric phase is stable for thicknesses down to 3 unit cells (1.2 nanometers). Our results imply that no thickness limit is imposed on practical devices by an intrinsic ferroelectric size effect.

Ferroelectricity is an example of the broad class of cooperative phenomena that includes superconductivity and ferromagnetism. For such phenomena, a different degree of ordering is expected to occur near surfaces or interfaces, leading to an intrinsic dependence on sample size. However, understanding size effects in ferroelectrics is complicated because polarization interacts more strongly than other order parameters with composition, strain, and charge, producing large extrinsic effects if these variables are uncontrolled. As a result, the size dependence of the paraelectric-to-ferroelectric phase transition remains an unresolved issue, in particular for the technologically important perovskites (*1*).

Research in this field has intensified recently (*2*–*13*) as a result of progress in the use of ferroelectric films, as well as concerns that intrinsic size effects may produce a fundamental limit to their performance. An increasingly wide range of applications are based on perovskite-structure ferroelectric thin films, including devices that rely on remnant polarization, such as nonvolatile memory elements (*14*), and devices that make use of the innate piezoelectric and pyroelectric properties of a ferroelectric, such as those found in microelectromechanical systems (*15*). The enormous technological potential of these materials depends on maintaining a stable ferroelectric phase as devices continue to be miniaturized. However, researchers have historically observed reduced polarization and lower paraelectric-to-ferroelectric transition temperatures (T_C) as size is reduced, and extrapolation has indicated that there is a critical size below which no ordering occurs. Moreover, size effects are expected to be largest when the polarization is normal to the film surface, which is the typically desired polarization direction in devices (*16*).

Several systematic studies of size effects have been carried out on powders processed to achieve small particles [(*11*, *17*) and references therein]. These studies have focused on the prototypical ferroelectric perovskite, $PbTiO_3$. The smallest particles studied, with diameters from 55 to 35 unit cells (1 unit cell ≈ 0.4 nm), showed suppressions of T_C of 14 to 50 K relative to the unstrained, stoichiometric bulk value (765 K). These data were extrapolated to predict a critical size at room temperature of 20 to 30 unit cells. Studies have also been carried out on epitaxial films (*4*, *9*, *13*, *18*), which can have better defined strain states. By combining electric force microscopy and piezoelectric scanning probe microscopy, Tybell *et al.* (*13*) demonstrated stable polarization in a $Pb(Zr_{0.2}Ti_{0.8})O_3$ film 10 unit cells thick at room temperature. Such experimental results have been discussed in terms of an intrinsic critical thickness by choosing values of coefficients in phenome-

[1]Materials Science Division, Argonne National Laboratory, Argonne, IL 60439, USA. [2]Department of Physics, Northern Illinois University, DeKalb, IL 60115, USA.

*To whom correspondence should be addressed. E-mail: stephenson@anl.gov